PAPER

Cooperative lone pair–π and coordination interactions in naphthalene diimide coordination networks†

Xin Fang,[ab] Xiong Yuan,[ab] Yan-Bo Song,[ab] Jun-Dong Wang[ab] and Mei-Jin Lin*[ab]

Lone pair–π interaction is an important but less studied binding force. Naphthalene diimides (NDIs) are ideal to form such an interaction because their quadrupole moment is exceptionally positive. Here, we report the combination of NDI ligands bearing two divergently oriented pyridyl units with different metal nitrates in different solvents resulting in six neutral 1-D coordination networks, in which the nitrate anions not only serve as capping ligands to coordinate to metal centers but also provide lone pairs to interconnect with the π-acidic NDI ligands through lone pair–π interactions. Interestingly, such lone pair–π interactions are found to have a synergic effect on the coordination interactions of the aforementioned NDI ligands with metal ions. In other words, metal-ion-directed self-assembly of NDI ligands is supposed to be driven by cooperative lone pair–π and coordination interactions.

Introduction

Non-covalent interactions involving aromatic rings play a crucial role in both chemical and biological systems, such as protein folding,[1] the DNA double helix,[2] enzyme–substrate complexes[3] and many supramolecular assemblies with artificial hosts.[4] As a result of this broad importance, numerous attempts have been made to elucidate and quantify these interactions, including π–π,[5] CH–π,[6] cation–π,[7] anion–π,[8] and lone pair–π interactions.[9] Among them, the lone pair–π interaction, which takes place between lone pair-bearing atoms in neutral molecules and electron-deficient π-acidic aromatic systems, is counterintuitive and interesting but less studied until Egli and Gessner firstly identified the important role of this interesting interaction in the Z-DNA structure.[10] Since then, it has received a great deal of interest both in theoretical chemistry[11] and in experimental areas.[12] Moreover, some receptors based on lone pair–π interactions have promising applications in π–Lewis acid catalysis.[13]

Naphthalene diimides (NDIs) are an attractive class of functional π-conjugated molecules bearing an exceptionally electron-deficient parent core,[14] which makes them have a strong tendency to interact with electron-rich lone pair-bearing atoms. As expected, the detailed analysis of the Cambridge Structure Database (CSD) has shown that numerous NDI structures have been found where carbonyl oxygen atoms are within 3.5 Å above the imide units. To our surprise, few of them involved coordination networks from N-containing rigid and conjugated NDI ligands.[15] Such NDI ligands generally possess very weak coordination abilities towards metal ions since the electron density of each pyridine moiety is withdrawn by their electron-deficient NDI core, which could be theoretically improved by the incorporation of electron-donating groups into the NDI core through a covalent approach.[14] Another possible strategy to increase the coordination abilities of the aforementioned NDI ligands is the addition of electron-rich species above the NDI core through the so-called anion–π or lone pair–π interactions.[16] Herein, we report that the lone pair–π and coordination interactions in NDI coordination networks are indeed synergic.

To validate the conjecture that lone pair–π interactions can enhance the coordination abilities of NDI ligands, we chose N,N′-di(4-pyridyl)-1,4,5,8-naphthalene diimide[15d,17] (DPNDI, Scheme 1) as a proof-of-concept ligand. When self-assembled with different metal nitrates, six 1-D coordination networks have been obtained, in which the nitrate anions not only serve as capping ligands to coordinate to metal centres but

a College of Chemistry, Fuzhou University, 350116, China
b State Key Laboratory of Structural Chemistry, Fujian Institute of Research on the Structure of Matter, CAS, 350002 China. E-mail: meijin_lin@fzu.edu.cn; Tel: 0086 591 2286 6143

† Electronic supplementary information (ESI) available: The detailed single crystal structures, PXRD, TGA as well as IR studies. CCDC 1008612, 987800–987801, 1008404–1008407. For ESI and crystallographic data in CIF or other electronic format see DOI: 10.1039/c4ce01233j

Scheme 1 Chemical structure of DPNDI.

also provide lone pairs to interconnect with the π-acidic DPNDI ligands through lone pair–π interactions. The X-ray single crystal diffraction analyses revealed that such lone pair–π interactions have a cooperative effect on the coordination abilities of DPNDIs. That is, the lone pair–π interactions are increased by the coordination interactions of DPNDIs at both extremities owing to the electron withdrawal by metal ions, and in turn they simultaneously enhance coordination interactions because of the electron donation from the oxygen lone-pair electrons of nitrate units to DPNDIs. This synergy is undoubtedly of considerable realistic significance not only for metal ion-directed self-assembly of NDI derivatives but also for the improvement of the π-acidity of the NDI based coordination networks that are ideal for the study of heterogeneous catalysis.

Experiments

Materials and measurements

N,N'-Dimethylacetamide (DMA, 99%), N-methylpyrrolidin-2-one (NMP, 99%), tetrahydrofuran (THF, 99.5%), diethyl ether and $Zn(NO_3)_2 \cdot 6H_2O$ (99%) were purchased from Sinopharm Chemical Company. The organic ligand N,N'-di(4-pyridyl)-1,4,5,8-naphthalene diimide (DPNDI) was synthesized following the reported process.[17] All chemicals and reagents were used as received unless otherwise stated. The infrared spectra have been measured in the range of 400–4000 cm^{-1} using a Perkin-Elmer FT-IR spectrophotometer. Powder X-ray diffraction (PXRD) patterns have been recorded using a Rigaku MiniFlex-II X-ray diffractometer, while thermogravimetric analyses (TGA) of crystalline samples have been performed using an STA 449C simultaneous thermal analyser.

Synthesis

$\{[Zn(DPNDI)(NO_3)_2(H_2O)] \cdot 3DMA\}_n$ (1: M = Zn, 2: M = Cu, and 3: M = Co). A mixture of DPNDI (50 mg, 0.12 mmol), $M(NO_3)_2 \cdot 6H_2O$ (0.12 mmol, M = Zn, Cu, or Co for complexes 1, 2, 3, respectively), and DMA (5 mL) was stirred for 1 hour, filtered, and then block crystals were grown by diffusion of diethyl ether into the filtrate under room temperature for days.

1: light yellow crystals, yield: 39% based on DPNDI. IR data (KBr, cm^{-1}): 3066(w), 2938(w), 1716(m), 1681(s), 1617(s), 1445(w), 1360(s), 1307(w), 1246(m), 1203(w), 1026(m), 873(w), 829(w), 759(m), 636(m), 592(w), 528(w).

2: green crystals, yield: 47% based on DPNDI. IR data (KBr, cm^{-1}): 3095(w), 2952(w), 1719(s), 1679(s), 1633(m), 1613(m), 1581(m), 1386(s), 1348(s), 1297(w), 1248(m), 1210(w), 1144(w), 1021(m), 866(w), 831(m), 759(m), 710(w), 641(m), 598(w), 532(m).

3: red crystals, yield: 53% based on DPNDI. IR data (KBr, cm^{-1}): 3076(w), 2941(w), 1719(s), 1679(s), 1610(m), 1579(w), 1449(w), 1389(s), 1346(s), 1308(w), 1251(m), 1206(w), 1146(w), 1018(w), 983(w), 871(w), 762(m), 716(m), 638(m), 601(w), 532(w).

$\{[M_{0.5}(DPNDI)_{0.5}(NMP)(NO_3)] \cdot {\sim}1NMP\}_n$ (4: M = Zn, 5: M = Cu, 6: M = Co). A mixture of DPNDI (50 mg, 0.12 mmol), $M(NO_3)_2 \cdot 6H_2O$ (0.12 mmol, M = Zn, Cu, or Co for complexes 4, 5, 6, respectively), and NMP (5 mL) was stirred for 1 hour, filtered, then block crystals were grown by diffusion of diethyl ether into the filtrate under room temperature for days.

4: brown crystals, yield: 39% based on DPNDI. IR data (KBr, cm^{-1}): 3603(m), 3066(w), 2937(w), 2885(w), 1676(vs), 1351(s), 1249(m), 1114(w), 1026(w), 981(w), 873(w), 760(m), 637(m), 533(w).

5: green crystals, yield: 34% based on DPNDI. IR data (KBr, cm^{-1}): 3059(w), 2939(w), 2877(w), 1613(w), 1581(w), 1610(m), 1504(w), 1446(w), 1386(m), 1351(s), 1300(w), 1251(s), 1116(w), 1064(w), 986(m), 871(w), 834(w), 770(m), 713(w), 641(m), 535(w).

6: light red crystals, yield: 57% based on DPNDI. IR data (KBr, cm^{-1}): 3057(w), 2935(w), 1710(s), 1670(s), 1641(s), 1604(w), 1585(w), 1502(w), 1425(m), 1357(s), 1311(s), 1259(s), 1110(w), 1039(w), 989(m), 871(w), 767(s), 719(m), 634(s), 582(w), 538(m).

X-ray diffraction analysis

Crystal data for DPNDI, 1, 4–6 were collected using graphite monochromatic Mo-Kα radiation (λ = 0.71073 Å) in ω scan mode with a RIGAKU R-AXIS RAPID IP diffractometer at 293 K, while those for 2 and 3 were collected using a Rigaku Saturn 724 CCD diffractometer with Mo Kα radiation (λ = 0.71073 Å) at 173 K. The structures were solved by the direct method and different Fourier syntheses. All calculations were performed by full-matrix least-squares methods on F^2 by using the SHELX-97 program;[18] all non-hydrogen atoms were refined with anisotropic thermal parameters and the hydrogen atoms were fixed at calculated positions and refined using a riding model. For complexes 3–6, some included solvents were disordered and thus their contributions were subtracted from the data using SQUEEZE from the PLATON package of the crystallographic software.[19] All of the crystal data and the structure refinements are summarized in Table 1. Crystallographic data have been deposited with the Cambridge Crystallographic Data Center (CCDC) as supplementary publication numbers CCDC 1008612, 987800–987801 and 1008404–1008407 for DPNDI, 4, 1, 2, 3, 5 and 6, respectively.

Results and discussion

Due to the strong π–π interactions, the starting material DPNDI is insoluble in common organic solvents but highly soluble in electron-rich solvents, such as DMF, DMA, and NMP. Its good solubility may not only be attributed to the high polarity of such solvents but is also related to the formation of lone pair–π interactions between the solvents and the NDI π-acceptors during dissolution. Indeed, the slow diffusion of THF into the DMF solution of DPNDI led to red prism crystals suitable for X-ray diffraction analysis, which revealed that each DPNDI molecule is stabilized by two DMF molecules—one above and another below the NDI plane—through lone pair–π interactions (Fig. 1). The distances

Table 1 Crystal data and structure refinement parameters for **1**–**6**[a],[b]

Complexes	DPNDI	1	2	3	4	5	6
Crystal size (mm)	0.36 × 0.22 × 0.21	0.35 × 0.25 × 0.21	0.43 × 0.40 × 0.28	0.39 × 0.28 × 0.21	0.40 × 0.32 × 0.22	0.34 × 0.28 × 0.21	0.49 × 0.38 × 0.29
Empirical formula	$C_{30}H_{26}N_6O_6$	$C_{36}H_{41}N_9O_{14}Zn$	$C_{36}H_{41}CuN_9O_{14}$	$C_{32}H_{32}CoN_8O_{13}$	$C_{34}H_{30}N_8O_{12}Zn$	$C_{34}H_{30}CuN_8O_{12}$	$C_{34}H_{30}CoN_8O_{12}$
Formula weight	566.57	889.15	887.32	795.59	808.03	806.20	801.59
Crystal system	Monoclinic	Triclinic	Triclinic	Triclinic	Tetragonal	Tetragonal	Tetragonal
Space group	$P21/c$	$P\bar{1}$	$P\bar{1}$	$P\bar{1}$	$I\bar{4}2d$	$I\bar{4}2d$	$I\bar{4}2d$
a (Å)	5.4543(11)	12.470(3)	12.355(3)	12.280(3)	19.586(3)	19.379(3)	19.642(3)
b (Å)	13.088(3)	12.614(3)	12.541(3)	12.491(3)	19.586(3)	19.379(3)	19.642(3)
c (Å)	19.406(4)	14.991(3)	14.681(3)	14.649(3)	24.077(5)	23.744(5)	23.896(5)
α (°)	90	91.74(3)	91.05(3)	91.44(3)	90	90	90
β (°)	93.39(3)	102.37(3)	102.88(3)	102.46(3)	90	90	90
γ (°)	90	116.90(3)	117.34(3)	115.88(3)	90	90	90
V (Å³)	1382.9(5)	2032.0(8)	1950.6(8)	1955.7(8)	9236(3)	8917(2)	9219(3)
Z	2	2	2	2	8	8	8
D_c (g cm⁻³)	1.361	1.453	1.511	1.351	1.162	1.201	1.155
μ (Mo Kα) (mm⁻¹)	0.097	0.682	0.641	0.509	0.590	0.551	0.431
$F(000)$	592	924	922	822	3328	3320	3304
Collected reflections	12 630	19 594	16 364	16 627	41 995	41 916	41 533
Independent reflections	3055	9096 (0.0400)	8609 (0.0356)	8654 (0.0429)	5289 (0.1006)	5093 (0.1004)	5276 (0.1054)
Goodness-of-fit on F^2	1.066	1.044	1.085	1.100	1.030	1.021	1.017
R_1[a], wR_2[b] ($I > 2\sigma(I)$)	0.0869, 0.2811	0.0582, 0.1462	0.0704, 0.1711	0.0661, 0.1577	0.0787, 0.2072	0.0913, 0.2315	0.0636, 0.1776
R_1[a], wR_2[b] (all data)	0.1097, 0.3107	0.0942, 0.1699	0.0754, 0.1755	0.0784, 0.1664	0.1172, 0.2292	0.1630, 0.2719	0.0733, 0.1843

[a] $R_1 = \sum ||F_o| - |F_c||/\sum |F_o|$. [b] $wR_2 = [\sum w(F_o^2 - F_c^2)^2/\sum w(F_o^2)]^{1/2}$.

between the oxygen lone-pair electrons in both the DMF molecules and the imide ring of DPNDI are around 3.14 Å.

To examine the effect of metal-ion coordination on the lone pair–π interactions, slow diethyl ether vapour diffusion into a DMA solution of DPNDI and zinc, copper and cobalt nitrates was performed, resulting in different coloured crystalline materials 1–3, respectively, after several days. For all three combinations, the structural studies were performed using an X-ray diffraction technique on single crystals which showed that they are isostructural and all of them crystallize in the triclinic $P\bar{1}$ space group (Tables S1–S6†). Here, the zinc complex is taken as an example for structural description. As shown in Fig. 2a, the four component system composed of DPNDI, water, a Zn^{2+} cation and an NO_3^- anion (triangular geometry with ONO angles of 120°) behaving as an inorganic ligand leads to the formation of a neutral zigzag architecture. In the architecture, each Zn^{2+} is saturated

by one O atom from a water molecule (d_{Zn-O} = 2.02 Å) and four O atoms from two NO_3^- anions (d_{Zn-O} = 2.16–2.54 Å) to generate a neutral distorted pentagonal complex, which further bridges the neighbouring two DPNDI units through the formation of Zn–N (d_{Zn-N} = 2.12–2.14 Å, ∠N–Zn–N = 171.7°) bonds in the axial direction of the metal resulting in the final 1-D neutral zigzag network. For each DPNDI, the dihedral angle between the NDI core and the pyridine group is around 72.0°, which is close to that for the free ligand (ca. 70.4°).

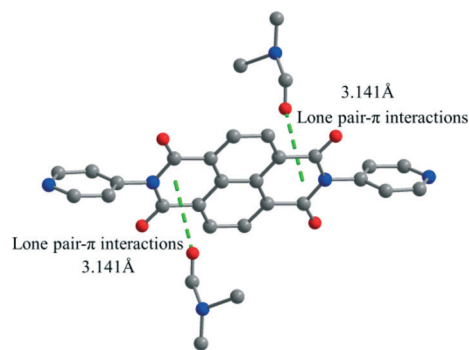Among the neighbouring linear networks, each smallest repetitive unit carries three DMA molecules: two of them

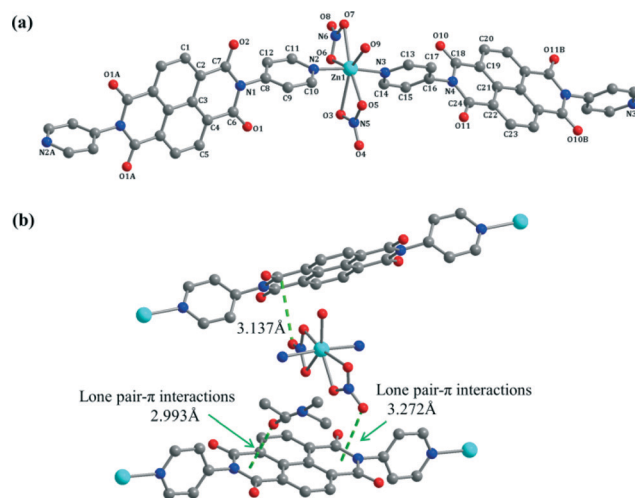**Fig. 1** Single crystal structure of free DPNDI highlighting the lone pair–π interactions.

Fig. 2 (a) Coordination environment of Zn^{2+} in complex **1** (symmetry codes: A: $-x$, $-y$, $-z$; B: $3 - x$, $3 - y$, $1 - z$.). (b) Lone pair–π interactions are highlighted in complex **1**.

are attached to the coordinated water through hydrogen bonds (Fig. S1†), while the other is coordinated to the imide ring of the DPNDI unit *via* a lone pair–π interaction (Fig. 2b). Interestingly, the distance between the oxygen lone-pair electrons in the DMA molecule and the imide ring is only 2.993 Å, much shorter than that found in the free ligand (3.141 Å). Similar shorter distances between the DMA molecules and the DPNDI units (2.94 Å) are also found in complex **2** whose solvents have not been subtracted from the data using SQUEEZE. Such enhanced lone pair–π interactions may be attributed to the increased π-acidity of DPNDI units resulting from the coordination interactions of the electron-poor metal cations which can withdraw some electrons from organic ligands. Although a similar propensity of nitrogen-containing ligands to interact with anions has already been demonstrated to be reinforced upon metal ion coordination in theoretical studies,[20] this is the first experimental evidence observed so far for naphthalene diimide derivatives. According to the theoretical calculations,[21] lone pair–π and coordination interactions in nitrogen-containing ligands are synergic, that is, the enhanced lone pair–π interactions in turn can also increase the strength of coordination interactions. Indeed, such a synergic effect has been observed in our coordination networks (see below).

Other than the aforementioned lone pair–π interactions, another kind of interplay between the coordinated NO_3^- anions and the DPNDI units can also be detected in all three complexes **1–3** (Fig. 2b and S2–S3†). The distances between the oxygen atoms of two coordinated NO_3^- anions and the imide rings are 3.14 and 3.27 Å for zinc complex **1**, 3.03 and 3.19 Å for copper complex **2**, and 3.15 and 3.28 Å for cobalt complex **3**. Recently, Saha and co-workers have reported similar interplays in a close zinc coordination network which were labelled as anion–π interactions.[22] Considering the charge neutralization by metal cations, the nitrate anions in the networks have already formed neutral metal nitrate complexes whose binding forces with DPNDI units are not pure anion–π interactions but are more likely to be lone pair–π interactions. Moreover, analysis of the crystallographic data for our network **1** and those reported by Saha[22] reveals that the DPNDI units with weak lone pair–π interactions with the coordinated NO_3^- anions in network **1** ($d_{O-\pi}$ = 3.14–3.27 Å) have a weak tendency to interact with metal ions ($d_{Zn–N}$ = 2.12–2.14 Å), while those in the literature with short lone pair–π distances (two kinds of lone pair–π interactions reported by Saha with $d_{O-\pi}$ = 2.90 or 3.01 Å, respectively) possess a strong propensity to coordinate to metal centers ($d_{Zn–N}$ = 2.08 or 2.10 Å, respectively). Thus, lone pair–π and coordination interactions are synergic.

To further corroborate our finding, more crystallographic evidence is required. Fortunately, the replacement of the crystallization solvent of **1–3**, DMA, with NMP leads to three new crystalline materials **4–6**. The X-ray single crystal diffraction analyses reveal that they are also isostructural but they crystallize in the tetragonal $I\bar{4}2d$ space group (Tables S7– S12†). In their crystal structures, each M^{2+} cation

is alternately coordinated by four O atoms from two NO_3^- anions ($d_{Zn–O}$ = 2.16 Å for **4**, $d_{Cu–O}$ = 2.21 Å for **5**, and $d_{Co–O}$ = 2.12 Å for **6**) and two NMP molecules ($d_{Zn–O}$ = 2.11 Å for **4**, $d_{Cu–O}$ = 2.07 Å for **5**, and $d_{Co–O}$ = 2.08 Å for **6**) in a square plane to form a neutral metal complex which interconnects two DPNDI tectons through coordination interactions ($d_{Zn–N}$ = 2.10 Å for **4**, $d_{Cu–N}$ = 2.00 Å for **5**, and $d_{Co–N}$ = 2.13 Å for **6**) to generate the final linear coordination networks (Fig. 3a). Due to the NO_3^- anions serving as monodentate ligands in the networks **4–6**, all of the interplays between the oxygen lone-pairs of the coordinated NO_3^- anions and the imide rings of DPNDI units ($d_{O-\pi}$ = 2.81, 2.91 and 2.81 Å, respectively; see Fig. 3b and S4–S5†) are shorter than those found in **1–3** (see above). As a result of such enhanced lone pair–π interactions, the anti-symmetric stretching vibrations of nitrate anions in **4–6** (see the experiments and Fig. S6;† 1351 cm^{-1}, 1351 cm^{-1} and 1357 cm^{-1} for **4–6**, respectively) are decreased compared to those in **1–3** (1360 cm^{-1}, 1386 cm^{-1} and 1389 cm^{-1} for **1–3**, respectively). Moreover, a comparison of the crystallographic data for our networks **1–6** indeed shows that the enhanced lone pair–π interactions between the coordinated NO_3^- anions and the DPNDI units in **4–6** slightly strengthen the interaction abilities of the latter towards metal cations.

The purity of the crystalline materials generated has been investigated by X-ray diffraction on powder samples in all six cases (Fig. S7†). The latter study revealed that almost only one phase was observed for the networks **1–6** because of a rather good fit between their simulated and observed patterns. The slight discrepancies may have come from the trace collapsed crystalline materials upon removal of the solvent molecules, which is further supported by their thermogravimetric analyses. The thermal behaviours of **1–4** have been investigated under a nitrogen atmosphere in
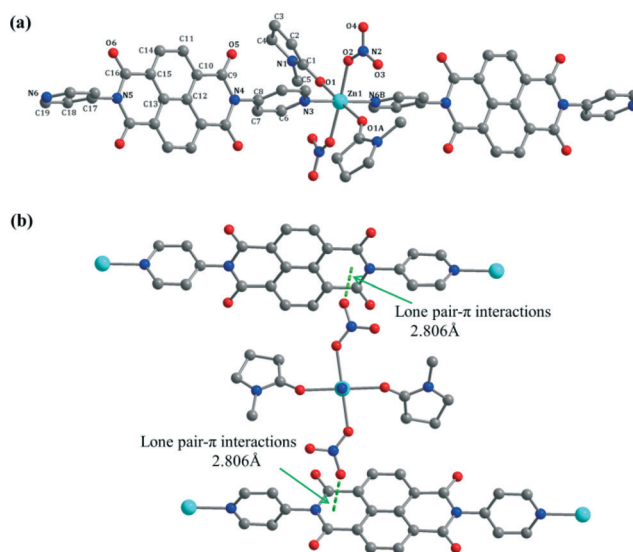

Fig. 3 (a) Coordination environment of Zn^{2+} in complex **4** (symmetry codes: A: *x*, −*y* + 1/2, −*z* + 1/4; B: −1 + *x*, *y*, *z*.). (b) Lone pair–π interactions are highlighted in complex **4**.

the temperature range of 40–800 °C. As shown in Fig. S8,† less than 2% weight losses were observed in **1–3** at 100 °C, while around 15% weight loss was observed in **4**; this is because **1–3** only included high boiling point DMA molecules while **4**, aside from NMP, might also contain some low boiling point solvents that are removed by using SQUEEZE during its structural refinement. In the temperature range of 100–200 °C, the *ca.* 25% weight loss in each network was attributed to the loss of crystalline solvents (calculated value: 29.3% for **1**, 29.4% for **2**, 21.9% for **3** and 24.5% for **4**). Then almost no weight loss was observed until about 250 °C for all four networks, which indicates that their frameworks are thermally stable. Unfortunately, no discernible effect of lone pair–π interactions on their thermal stability could be observed.

Conclusions

In summary, the combination of the electron-deficient DPNDI ligand with different metal nitrates in different solvents led to six neutral 1-D coordination networks, in which the nitrate anions not only serve as capping ligands to connect with metal centers but also provide oxygen lone pairs to bridge to the π-acidic DPNDI units through lone pair–π interactions. Interestingly, such lone pair–π interactions have been demonstrated to have a synergic effect on the coordination interactions of DPNDI with metal ions. In other words, metal ion directed self-assembly of DPNDI is supposed to be driven by cooperative lone pair–π and coordination interactions. This finding is of considerable realistic significance not only for metallosupramolecular self-assembly of NDI derivatives, but also for the development of NDI based π-acid catalysts.

Acknowledgements

Notes and references

1 S. K. Burley and G. A. Petsko, *Science*, 1985, **229**, 23–28.
2 R. Bhattacharyya, U. Samanta and P. Chakrabarti, *Protein Eng.*, 2002, **15**, 91–100.
3 (*a*) E. A. Meyer, R. K. Castellano and F. Diederich, *Angew. Chem., Int. Ed.*, 2003, **42**, 1210–1250; (*b*) L. M. Salonen, M. Ellerman and F. Diederich, *Angew. Chem., Int. Ed.*, 2011, **50**, 4808–4842.
4 J.-M. Lehn, *Supramolecular Chemistry: Concepts and Perspectives*, VCH, Weinheim, 1995.
5 C. Janiak, *J. Chem. Soc., Dalton Trans.*, 2000, 3885–3896.
6 (*a*) M. Nishio, Y. Umezawa, M. Hirota and Y. Takeuchi, *Tetrahedron*, 1995, **51**, 8665–8701; (*b*) M. Nishio, M. Hirota and Y. Umezawa, *The CH/π Interaction. Evidence, Nature, and Consequences*, Wiley-VCH, New York, 1998; (*c*) M. Brandl, M. S. Weiss, A. Jabs, J. Sühnel and R. Hilgenfeld, *J. Mol. Biol.*, 2001, **307**, 357–377.
7 (*a*) D. A. Dougherty, *Science*, 1996, **271**, 163–168; (*b*) J. C. Ma and D. A. Dougherty, *Chem. Rev.*, 1997, **97**, 1303–1324; (*c*) R. S. Prajapati, M. Sirajuddin, V. Durani, S. Sreeramulu and R. Varadarajan, *Biochemistry*, 2006, **45**, 15000–15010; (*d*) Y.-J. Huang, Y.-B. Jiang, S. D. Bull, J. S. Fossey and T. D. James, *Chem. Commun.*, 2010, **46**, 8180–8182.
8 (*a*) B. L. Schottel, H. T. Chifotides and K. R. Dunbar, *Chem. Soc. Rev.*, 2008, **37**, 68–83; (*b*) A. Robertazzi, F. Krull, E.-W. Knapp and P. Gamez, *CrystEngComm*, 2011, **13**, 3293–3300; (*c*) A. Frontera, P. Gamez, M. Mascal, T. J. Mooibroek and J. Reedijk, *Angew. Chem.*, 2011, **123**, 9736–9756 (*Angew. Chem., Int. Ed.*, 2011, **50**, 9564–9583); (*d*) H. T. Chifotides and K. R. Dunbar, *Acc. Chem. Res.*, 2013, **46**, 894–906; (*e*) D.-X. Wang and M.-X. Wang, *J. Am. Chem. Soc.*, 2013, **135**, 892–897; (*f*) P. Gamez, *Inorg. Chem. Front.*, 2014, **1**, 35–43.
9 (*a*) M. Egli and S. Sarkhel, *Acc. Chem. Res.*, 2007, **40**, 197–205; (*b*) T. J. Mooibroek, P. Gamez and J. Reedijk, *CrystEngComm*, 2008, **10**, 1501–1515.
10 M. Egli and R. V. Gessner, *Proc. Natl. Acad. Sci. U. S. A.*, 1995, **92**, 180–184.
11 (*a*) I. Alkorta, I. Rozas and J. Elguero, *J. Org. Chem.*, 1997, **62**, 4687–4691; (*b*) S. Kawahara, S. Tsuzuki and T. Uchimaru, *Chem. – Eur. J.*, 2005, **11**, 4458–4464; (*c*) B. W. Gung, Y. Zou, Z. Xu, J. C. Amicangelo, D. G. Irwin, S. Ma and H.-C. Zhou, *J. Org. Chem.*, 2008, **73**, 689–693; (*d*) A. Jain, V. Ramanathan and R. Sankararamakrishnan, *Protein Sci.*, 2009, **18**, 595–605; (*e*) A. Bauzá, D. Quiñonero, P. M. Deyà and A. Frontera, *Comput. Theor. Chem.*, 2012, **998**, 20–25.
12 (*a*) T. Korenaga, T. Shoji, K. Onoue and T. Sakai, *Chem. Commun.*, 2009, 4678–4680; (*b*) J. S. Costa, A. G. Castro, R. Pievo, O. Roubeau, B. Modec, B. Kozlevčar, S. J. Teat, P. Gamez and J. Reedijk, *CrystEngComm*, 2010, **12**, 3057–3064; (*c*) J. Zukerman-Schpector, A. Otero-de-la-Roza, V. Luaña and E. R. T. Tiekink, *Chem. Commun.*, 2011, **47**, 7608–7610; (*d*) A. Das, S. R. Choudhury, C. Estarellas, B. Dey, A. Frontera, J. Hemming, M. Helliwell, P. Gamez and S. Mukhopadhyay, *CrystEngComm*, 2011, **13**, 4519–4527.
13 (*a*) N. Tanaka and Y. Masaki, *Synlett*, 2000, 406–408; (*b*) N. Tanaka, T. Miura and Y. Masaki, *Chem. Pharm. Bull.*, 2000, **48**, 1010–1016; (*c*) Y. Masaki, K. Yamazaki, H. Kawai, T. Yamada, A. Itho, Y. Arai and H. Furukawa, *Chem. Pharm. Bull.*, 2006, **54**, 591–593; (*d*) Y. Masaki, T. Yamada, H. Kawai, A. Itoh, Y. Arai and H. Furukawa, *Synlett*, 2006, 288–290.
14 (*a*) S. V. Bhosale, C. H. Jani and S. J. Langford, *Chem. Soc. Rev.*, 2008, **37**, 331–342; (*b*) N. Sakai, J. Mareda, E. Vauthey and S. Matile, *Chem. Commun.*, 2010, **46**, 4225–4237; (*c*) F. Würthner and M. Stolte, *Chem. Commun.*, 2011, **47**, 5109–5115; (*d*) S. V. Bhosale, S. V. Bhosale and S. K. Bhargava, *Org. Biomol. Chem.*, 2012, **10**, 6455–6468.

15 (a) B. Q. Ma, K. L. Mulfort and J. T. Hupp, *Inorg. Chem.*, 2005, **44**, 4912–4914; (b) K. Hirai, H. Uehara, S. Kitagawa and S. Furukawa, *Dalton Trans.*, 2012, **41**, 3924–3927; (c) Q. X. Yang, L. F. Huang, M. D. Zhang, Y. Z. Li, H. G. Zheng and Q. Y. Lu, *Cryst. Growth Des.*, 2013, **13**, 440–445; (d) S. Guha, F. S. Goodson, R. J. Clark and S. Saha, *CrystEngComm*, 2012, **14**, 1213–1215.

16 (a) A. Frontera, P. Gamez, M. Mascal, T. J. Mooibroek and J. Reedijk, *Angew. Chem., Int. Ed.*, 2011, **50**, 9564–9583; (b) P. Gamez, *Inorg. Chem. Front.*, 2014, **1**, 35–43.

17 S. Guha, F. S. Goodson, L. J. Corson and S. Saha, *J. Am. Chem. Soc.*, 2012, **134**, 13679–13691.

18 G. M. Sheldrick, *Acta Crystallogr., Sect. A: Found. Crystallogr.*, 2008, **64**, 112–122.

19 A. L. Spek, *J. Appl. Crystallogr.*, 2003, **36**, 7–13.

20 D. Quiñonero, A. Frontera and P. M. Deyà, *ChemPhysChem*, 2008, **9**, 397–399.

21 A. Bauzá, D. Quiñonero, P. M. Deyà and A. Frontera, *Theor. Chem. Acc.*, 2012, **131**, 1219–1230.

22 A. Mitra, C. T. Hubley, D. K. Panda, R. J. Clark and S. Saha, *Chem. Commun.*, 2013, **49**, 6629–6631.